Submitted to Operations Research

Reshaping National Organ Allocation Policy

Theodore Papalexopoulos,[1] James Alcorn,[2] Dimitris Bertsimas,[1]
Rebecca Goff,[2] Darren Stewart,[3] Nikolaos Trichakis[1]
1. Operations Research Center, Massachusetts Institute of Technology, Cambridge, MA 02139
2. United Network for Organ Sharing, Richmond, VA 23219
3. NYU Grossman School of Medicine, New York, NY 10016

The Organ Procurement & Transplantation Network (OPTN) initiated in 2018 a major overhaul of all U.S. deceased-donor organ allocation policies, aiming to gradually migrate them to a so-called continuous-distribution model, with the goal of creating an allocation system that is more efficient, more equitable, and more inclusive. Development of policies within this model, however, represents a major challenge, as multiple efficiency and fairness objectives need to be delicately balanced. We introduce a novel analytical framework that leverages machine learning, simulation, and optimization to illuminate policy tradeoffs and enable dynamic exploration of the efficient frontier of policy options. In collaboration with the OPTN, we applied the framework to design a new national allocation policy for lungs. Since March 9, 2023, all deceased-donor lungs in the U.S. are allocated according to this policy that we helped design, projected to reduce waitlist mortality by approximately 20% compared to current policy based on simulations. We discuss how we extended our collaboration with the OPTN to the redesign of kidney, pancreas, heart and liver allocation, and how our framework can be applied to other application domains, such as school choice or public housing allocation systems.

Key words: fairness; policy design; multiobjective optimization; resource allocation; fairness and efficiency tradeoff; organ allocation

1. Introduction

In 2018, U.S. policymakers launched a program to redesign all U.S. deceased-donor organ allocation policies, and migrate them to a new so-called continuous distribution framework that will radically change the way organs from deceased donors are offered to candidates on the waiting list for transplantation. The vision behind this generational change is to create an allocation system that is more efficient, more equitable, and more inclusive. Designing allocation policies for such invaluable societal goods, however, represents a major challenge, as multiple efficiency and fairness objectives need to be delicately balanced, with different stakeholders often having disparate value judgments. In this work, we introduce a novel analytical framework that leverages machine learning, simulation, and optimization

to illuminate policy tradeoffs and enable dynamic exploration of the efficient frontier of policy options. In collaboration with U.S. policymakers, we applied our framework to the design of a new national allocation policy for lungs, playing an instrumental role in guiding the development process. Since March 9, 2023, all deceased-donor lungs in the U.S. are allocated according to a policy that we helped design, promising to reduce waitlist mortality by 20%, approximately, compared to current policy based on simulation projections. Based on this success, we have extended this collaboration and are now working towards the redesign of kidney, pancreas, heart and liver allocation. This highlights the potential of our framework to help reshape allocation policy for all other organs in the U.S., and have a positive and equitable impact on patient welfare for years to come.

In response to growing evidence that the extant organ allocation system might no longer best serve patients' needs (Section 2.2), the Organ Procurement & Transplantation Network (OPTN) made a landmark decision in 2018 to gradually migrate all of its allocation policies to a new framework termed "continuous distribution" (OPTN 2018). Within this framework, transplant candidates on the national waitlist will be ranked according to a scoring rule. The selection of key policy parameters, namely the score components and their associated weights, poses a challenging, multi-objective optimization problem with far-reaching ethical and practical implications. Given the limited supply of available organs, policies should seek to distribute organs to those most in need, over as broad a geographic area as feasible, while also safeguarding equity in access for different communities.

Crucially, policymakers must reconcile the views of a large and diverse set of stakeholders who often champion different tradeoffs. Some transplant professionals might favor local transplants, for example, aiming to reduce the potentially detrimental effects of longer organ transport times, while others might favor broader distribution to reach more medically urgent candidates who are farther away. Federal regulation, in the form of a "Final Rule" governing transplant policy (DHHS 2000), provides nonnegotiable, but often imprecise, guardrails, such as limitations on the extent to which geography can be incorporated into the ranking algorithm. Similar debates arise in calibrating pediatric priority, or in reducing access disparities based on race, birth sex, age, blood group, etc.

Adjudicating such debates in a rigorous manner necessitates the development of flexible decision support tools that can shed light on relevant tradeoffs and promote convergence towards more effective and inclusive allocation policies. To this end, we introduce a novel

framework for policy design based on multi-objective optimization. At a high level, we use machine learning and mixed-integer representable surrogate optimization models to approximate allocation outcomes, allowing us to characterize the (approximate) efficient frontier of policy design decisions. By varying the objective and constraints of the optimization, one can design policies with different efficiency and fairness characteristics. The result is a flexible decision-support tool that enables stakeholders, even those without technical expertise, to quickly iterate on different policy scenarios and refine their value judgments on relevant tradeoffs as they engage in the policy-making process.

We applied our methodology to the design of a continuous distribution policy for lung allocation, working closely with the OPTN Lung Transplantation Committee (LTC) and the United Network for Organ Sharing (UNOS). Using our optimization tool, we conducted several tradeoff analyses that helped guide the committee's decision-making process (LTC 2021a,b). In particular, the committee's official continuous distribution proposal used values for policy parameters that were identified as 'critical' points in our analysis for organ placement efficiency and pediatric priority. The proposal was distributed for public comment in August of 2021 (LTC 2021d), ratified in October of the same year (LTC 2021c), and approved by the OPTN Board of Directors in December 2021 (OPTN 2021b). It was implemented as national policy on March 9, 2023, guiding how lungs are allocated in the U.S. for years to come. We perform simulation studies that suggest the new policy could reduce waitlist mortality by 20%, approximately, compared to the status quo, averting 62 waitlist deaths per year, while also improving fairness and equity. Independent simulations performed by the Scientific Registry of Transplant Recipients (SRTR) place the estimated reduction of mortality at 40%, or 87 waitlist deaths averted per year (SRTR 2021a).

We believe these results demonstrate our framework's practicability and that it can be further applied to develop continuous distribution policies for other organs, as well as reshape how allocation policy is developed more generally. Indeed, based on this success, we are extending our collaboration with UNOS and are now working jointly for the redesign of kidney, pancreas, heart and liver allocation. Beyond organ transplantation, we also discuss how the general policy design framework we develop can be applied to other application domains, such as school choice or public housing allocation systems.

From a methodological standpoint, the paper contributes to the fields of multiobjective and black-box optimization. A single instance of black-box optimization is typically

in and of itself computationally expensive to solve, as extant methods require repeated calls to the 'black box' to approximate gradients. For black-box optimization problems with multiple objectives, one needs to solve a very large number of instances to elicit Pareto tradeoff curves, so a different line of attack is needed. The novel framework that we develop addresses these issues: it relies on surrogate models that are mixed-integer representable, and therefore allows approximately solving black-box optimization problems at scale, enabling tradeoff analyses under multiple objectives.

2. Organ Allocation in the United States

2.1. Background

In the U.S., all transplantation activities are overseen by the Organ Procurement & Transplantation Network (OPTN), which since 1986 has been operated under federal contract by the United Network for Organ Sharing (UNOS). Any patient seeking an organ transplant is registered on a national waitlist maintained by the OPTN. When an organ is recovered from a deceased donor, all candidates are ranked based on a fixed set of rules (the allocation policy) and the organ is offered sequentially until a candidate accepts.

The guiding principles for developing organ allocation policy are set forth by the OPTN Final Rule (DHHS 2000). Among other requirements, the Final Rule states that organ allocation policies must be based on "sound medical judgment," seek to achieve the "best use" of donated organs, and promote "efficient management" of organ placement. Allocation policies must aim to equitably distribute organs to those most in need, over as broad a geographic area as feasible. Translating these abstract ethical principles into concrete policy presents many ethical dilemmas for the transplant community. For example, what if one candidate would be transplanted at a hospital closer to the donor's location, reducing potentially detrimental effects of increased organ ischemic time and improving organ placement efficiency, but another, more distant candidate is sicker and likely to die sooner? Which of these two patients should an organ be offered to first?

Crucially, UNOS does not unilaterally determine allocation policy, but rather serves as a convener of the transplant community to help develop new and refine existing policy (OPTN 2021a). This community consists of transplant surgeons, physicians, Organ Procurement Organization professionals, transplant candidates and recipients, living donors and donor families, as well as the general public. Transplant professionals and patients provide input by serving on OPTN Committees that meet regularly to discuss the clinical and

practical details involved in developing policy. Committees work with UNOS to perform quantitative and qualitative analyses, solicit input from key constituencies, and formulate proposals to change how allocation works. These proposals are distributed to the broader community for public comment and possibly refined as a result, before being presented to the OPTN Board of Directors for final approval.

2.2. Continuous Distribution

Extant organ allocation policies operate within a classification-based framework, whereby candidates are separated into "similar" groups and each group assigned a distinct priority level (with additional ranking rules defined within each group, OPTN (2021c)). For example, an organ from a pediatric donor might be offered first to all pediatric candidates within some fixed distance of the donor hospital, ordered by their time on the waitlist. If none accepts, the organ is then offered to high-urgency adult candidates within the same boundary, followed by pediatric candidates who are farther away, and so forth. Such classification-based allocation systems have long been criticized as being unfair, particularly as regards to geographic distribution, since candidates' access to organs can vary highly depending on their inclusion or not in a particular group (Deshpande et al. 2017, Massie and Roberts 2018, Glazier 2018, Yang et al. 2020, Moore and Weimer 2021). Further, under such systems, often a single attribute, such as distance, might become the sole priority determinant.

With the central aim of increasing transparency and removing hard geographic (and other types of) boundaries that sometimes preclude organs from going to candidates most in need, the OPTN has recently embarked on a large-scale initiative to migrate all allocation policies—starting with lungs—from the current classification-based system to a borderless Continuous Distribution (CD) framework (LTC 2019). For exposition purposes, we will introduce the CD framework in the context of lung allocation, using the OPTN Lung Transplantation Committee's recent development process as a reference, but the general principles apply to all organs.

Under the CD paradigm, all candidates on the waitlist are prioritized according to a scoring rule. Relevant candidate and donor attributes are combined into a single Composite Allocation Score (CAS) which precisely determines a candidate's waitlist rank for the given organ. The two primary design decisions involved in developing such a policy are (1) what

patient and donor attributes should be included as score components in the CAS and with what functional form, and (2) their relative weighting in the composite score. Typically there is broad consensus on the former, while the latter is a central point of debate given its importance in balancing different policy objectives (Section 2.3).

As regards to the first design decision, the Lung Transplantation Committee's initial CD development process determined that the following patient and donor attributes would be included in the lung CAS:

- Post-transplant outcomes (PTAUC, "Post-Transplant Area Under (the survival) Curve"), a survival analysis-based measure of how long a patient is expected to live if they receive a transplant of median quality.
- Medical urgency (WLAUC, "Waitlist Area Under (the survival) Curve"), a survival analysis-based measure of how long a patient is expected to live if they do not receive a transplant and remain on the waitlist.
- Placement efficiency, a function of distance between the donor and recipient hospitals, reflecting the resources needed to match, transport and transplant the organ.
- Biological disadvantage points for candidates who are medically harder to match based on blood type, height and immune system sensitization level.[1]
- Patient access points for pediatric patients (aged < 18 years) and prior living donors.

Of note, the different attributes measure vastly different quantities in different units, making the problem of identifying appropriate relative weights challenging, which we discuss next. More details on the selected attributes and how they are measured can be found in the committee's proposal (LTC 2021d).

The second design decision, and focus of this work, is the selection of a set of relative weights for each attribute. Whenever an organ o becomes available, each compatible candidate p is assigned a vector $a_{o,p} \in \mathbb{R}^m$ reflecting their priority across of each of the m aforementioned attributes. To create a scoring rule, we seek a vector of score weights $\lambda \in \mathbb{R}^m$ so that $\text{CAS}_{o,p} = \sum_m \lambda_m a_{o,p,m}$. We next focus on why selecting these weights is an exceedingly difficult problem.

2.3. Challenges in Designing Policy

The selection of score weights presents two key challenges. First, it is fundamentally a multi-objective problem, in which policymakers must strike a balance between multiple

efficiency, utility and fairness-related objectives. Moreover, different stakeholders might champion different tradeoffs in these objectives that must be reconciled during the development process. Second, given a vector of score weights, predicting policy outcomes under counterfactual allocation is challenging in and of itself, and requires, in this context, complex simulations to capture the many interacting effects of a given prioritization scheme. Simulation is both computationally expensive and non-transparent, making it hard to anticipate what outcomes would result for a given policy, or how they would compare across different proposals.

In the case of continuous distribution, the score weights are the primary levers through which policymakers can influence tradeoffs to meet the Final Rule's many utility (mortality and post-transplant outcomes), efficiency (transport burden and costs), and fairness (equity in access to organs) mandates. For example, placing a low relative weight on placement efficiency results in policies that favour broad geographic distribution to highly urgent or otherwise disadvantaged patients, but might exhibit worse post-transplant outcomes as organs need to be transported longer distances. Similarly, a higher weight on biological disadvantage might result in more equitable distribution to patients who are medically harder to match, but increase waitlist mortality as organs are not allocated to the most severely ill patients.

Given a set of scoring attributes then, their weights should ideally be chosen to reflect the community's consensus value judgments on the importance of different utility, equity, and efficiency considerations. Since different stakeholders often champion different tradeoffs, the OPTN's policy development process is designed to foster wide-ranging, evidence-based discussion on tradeoffs and solicit input from the community's many and diverse constituencies (OPTN 2021a).

Simulation modeling plays an integral role in this process by allowing stakeholders to assess policy proposals across a wide range of metrics. The Simulated Allocation Models (SAMs), developed and maintained by the Scientific Registry of Transplant Recipients (SRTR), use historical waitlist and transplant data to simulate counterfactual allocation under a proposed policy, e.g., a continuous distribution with given weights (SRTR 2021b). SAMs use discrete event simulation to predict system-wide outcomes such as:

- Waitlist and post-transplant mortality rate.
- Transplant and discarded organ rate.

- Disparities in the above among patient subpopulations, e.g., by age, geography, birth sex, race.
- Transportation efficiency metrics, e.g., median organ transport distance or % of organs flown.

While this ability to compare policy options across multiple metrics facilitates "outcome-driven" policy debates, the blackbox nature of the simulator introduces a significant challenge in selecting score weights. The mapping of weights to simulated outcomes is both computationally expensive and non-transparent, rendering optimization over them particularly challenging. In other words, it is hard to anticipate what the simulated outcomes would be for a given set of weights—which in turn makes it hard to find what weights would achieve a desired balance in multiple objectives.

The OPTN committees' simulation modeling has typically been conducted via trial-and-error, with simulated outcomes from initial policy ideas used to iteratively refine those ideas until acceptable predicted outcomes are achieved. The time-consuming process of iteratively running simulations, reviewing and discussing results, and determining the next set of options to simulate means that this crucial evidence-generating phase of policy development can consume many months or even years. Worse, the limited number of options that can be simulated might not reflect the full range of tradeoffs, while often it is difficult to identify what, if any, proposed remedy would achieve some desired improvement during an iteration. The decade-long development of the kidney allocation system (KAS), in which well over 30 different policy options were simulated, is a prime example (Stegall et al. 2017, RFI 2008).

3. Optimization Framework

In this work, we introduce a general optimization-based framework for policy design that seeks to address the two challenges we discussed in the previous section, namely (i) that predicting a policy's outcomes is the result of some complex, non-transparent process that complicates optimization, and (ii) that policymakers seek to balance tradeoffs in multiple objectives, reconciling potentially disparate value judgments from diverse stakeholders. To facilitate exposition, we introduce our methodology in the context of continuous distribution for lung allocation; however, the model we develop can be applied more generally for the design of any type of parametrized policy, be it in organ allocation or beyond (see relevant discussion in Section 5).

The basic building block of our framework is an approach to solve what is essentially an inverse control problem: given a set of desired outcomes, our model seeks the policy parameters that best achieve them. We use machine learning to predict allocation outcomes, allowing us to bypass explicit simulation during optimization. As a result, policymakers can directly design policies with given efficiency/fairness characteristics, in near real-time, unconstrained by the expensive, non-transparent simulator. Moreover, this more efficient optimization enables outcome-driven tradeoff analysis by varying the optimization objective and constraints. The result is a flexible decision support tool for policymakers, including those with non-technical backgrounds, to evaluate policy tradeoffs and understand the impact of design decisions on their outcomes of interest.

3.1. Mathematical Model

We consider a function $B : \mathcal{X} \mapsto \mathcal{Y}$, with $\mathcal{X}$ a bounded domain and $\mathcal{Y} \subseteq \mathbb{R}^d$. The domain $\mathcal{X}$ represents the set of valid policy parameter settings, e.g., possible score weights λ for a continuous distribution allocation policy. For the purposes of optimization, we require that $\mathcal{X}$ is Mixed-Integer Linear Programming (MILP) representable; that is, it can be expressed in terms of continuous- and integer-valued decision variables and linear inequality constraints on them. The multi-dimensional output $\mathcal{Y}$ encodes a set of d outcomes that may be of interest to decision-makers, e.g., mortality rate, transplant rate, transport burden, equity metrics, etc. We assume without loss of generality that lower values are preferable for all outcomes (negating the sign of the outcome if necessary).

The function B is not assumed to have known functional form, and may only be queried at particular inputs $x \in \mathcal{X}$ to observe $y = B(x)$. Such functions are typically referred to as "blackbox" functions, in the sense that they do not provide explicit gradients or structural properties that might aid in optimization over $\mathcal{X}$. Moreover, they are typically computationally expensive to evaluate, which renders finite-difference gradient methods impractical to run at large scale. In lung allocation for example, B would represent the counterfactual allocation simulator that predicts transplant outcomes for a given parametrized policy.

We now define the concept of a *problem instance* on the function B; that is, an optimization problem over $\mathcal{X}$ with a fixed set of outcomes appearing in the objective and constraints. For lung allocation, a problem instance might correspond to, say, finding the score weights λ that minimize waitlist mortality (primary outcome), with pre-specified upper bounds on

organ transport distance and transplant rate disparities (constrained outcomes). Mathematically, a problem instance $\pi = (j, \boldsymbol{b})$ consists of (i) a *primary objective* index $j \in [d]$ and (ii) a *requirement* vector $\boldsymbol{b} \in \mathbb{R}^d$, inducing the following optimization problem:

$$\begin{aligned} \underset{\mathbf{x}\in\mathcal{X}}{\text{minimize}} \quad & B_j(\mathbf{x}) \\ \text{subject to} \quad & B_i(\mathbf{x}) \leq b_i \quad \forall\, i \neq j. \end{aligned} \tag{$P(\pi)$}$$

The primary objective is the index of an outcome to be minimized directly. Other outcomes appear in the constraints, with right-hand side given by the requirement vector $\boldsymbol{b}$. Individual outcome requirements b_i are allowed to be $+\infty$, to denote that the outcome should be unconstrained.

Crucially, the set of problem instances of interest to the decision makers is not known a priori, and may change as they explore the space of solutions and achievable outcomes. If B is computationally expensive, sequentially solving multiple instances as users refine their requirements and explore tradeoffs quickly becomes impractical. This serves as a primary motivation for our work; we seek an efficient tool to compute solutions to arbitrary problem instances, or provide reasonable alternative solutions should those prove infeasible.

3.2. Methodology

Our approach, which comprises three phases, relies on surrogate modeling techniques (Koziel and Leifsson 2013) to formulate tractable approximations of $P(\pi)$. First, in the *Sample Design* phase, we generate a sample of representative inputs and evaluate each using the blackbox function B. The paired inputs and outputs serve as a supervised machine learning dataset, which is used to train high-fidelity, mixed-integer representable surrogate models of B during the *Surrogate Modeling* phase. Third, in the *Optimization* phase, we dynamically formulate and solve Mixed-Integer Linear Programs (MILP) to solve $P(\pi)$ for various instances π, using the surrogate models in lieu of B.

3.2.1. Sample Design In this phase, we query B at a representative sample of N design points and track the vector of outcomes, to be used in training of downstream surrogate models. We denote this dataset by $\{\mathbf{x}^n, \mathbf{y}^n = B(\mathbf{x}^n)\}_{n=1}^N$, with $\mathbf{x}^n \in \mathcal{X}$ and $\mathbf{y}^n \in \mathcal{Y}$ for all n. Concretely, in the lung allocation setting each datapoint would correspond to a randomly sampled set of scoring weights λ, as well as the vector of simulated outcomes using the corresponding scoring rule.

We sample each $\mathbf{x}^n$ uniformly from $\mathcal{X}$ to ensure broad generalization of the surrogate models across the domain. The problem of sampling uniformly from different domains is well studied in the experimental design literature, e.g., Latin hypercube sampling for hyper-rectangles (McKay et al. 1979), custom samplers for structured polyhedral sets like the unit simplex (Smith and Tromble 2004), or hit-and-run methods for more general polyhedral sets (Zabinsky and Smith 2013).

The choice of the sample size N represents the following tradeoff: a higher value could improve the quality of interpolation in the next step, but also increases computational burden through repeated queries of B. In practice, these queries are independent and can often be effectively parallelized to reduce overall computational time. More generally, the sample size choice is dependent on the application, and the form of $\mathcal{X}$ and B in particular. An effective way to navigate this choice, which we also followed in the organ policy application, is an iterative process between phases one and two: samples are generated and the out-of-sample fit of the surrogate model in the next phase is evaluated, e.g., through measuring out-of-sample performance. If the latter is deemed unsatisfactory, more samples are generated and added to the training set.

3.2.2. Surrogate Modeling Using the dataset $\{\mathbf{x}^n, \mathbf{y}^n\}_{n=1}^N$, we train machine learning models to predict each individual outcome; that is, parametric approximations $f_i(\mathbf{x}\,;\,\boldsymbol{\theta}^i) \approx B_i(\mathbf{x})$ for each outcome $i \in [d]$. Parameters $\boldsymbol{\theta}^i$ are estimated by minimizing an application-specific loss function, e.g., least-squares error, over the training set, and using cross-validation to select between different models for each outcome. We evaluate goodness-of-fit based on R^2 on a held-out test set, and retrain on the entire dataset to better interpolate the sampled design points.

For the choice of the parametric class for the surrogate models, note that since the models will be optimized over in the next phase, we require that their form is mixed-integer representable in the design variables $\mathbf{x}$. MILP formulations have been studied for a broad range of machine learning methods with varying power and complexity, including regression trees, tree-based ensembles, and neural networks (Biggs et al. 2017, Mišić 2020, Anderson et al. 2020, Maragno et al. 2021). Besides this requirement, the choice of the parametric class should balance the need for high predictive power (for accurate approximation) and low parametric complexity (for efficient optimization over the trained models in the next phase). The machine learning literature could also provide valuable insights

to navigate this choice (Murphy 2012). For example, it is usually preferable to start with a simple model, use cross-validation to evaluate the performance of different models, add complexity if necessary. In our implementation, we found that relatively simple piece-wise linear functions achieved very high accuracy while allowing for near real-time optimization (see Section 4.1).

Similar considerations could guide the choice of the loss function used to fit the model. As it is usually the case, it is important to experiment with different loss functions, hyperparameter tuning, and iterate until the model performs well for the specific problem and data (Murphy 2012). Some additional considerations could be sensitivity to outliers: depending on the nature of the data, a loss function that is less sensitive to outliers might be preferable; for example, in the absence of outliers, mean squared error could work well, whereas in the presence of outliers, mean absolute error or Huber loss would be preferable as they tend to be less sensitive to outliers. Finally, if sparsity is desirable, compatible loss functions such as mean absolute error could be preferable.

3.2.3. Optimization Phase In the optimization phase, given any problem instance π, we solve a surrogate optimization problem to find an approximate solution to $P(\pi)$, by replacing B with the trained approximations:

$$\begin{aligned} \underset{\mathbf{x}\in\mathcal{X}}{\text{minimize}} \quad & f_j(\mathbf{x}\,;\,\boldsymbol{\theta}^j) \\ \text{subject to} \quad & f_i(\mathbf{x}\,;\,\boldsymbol{\theta}^i) \le b_i \quad \forall\, i. \end{aligned} \tag{$S(\pi)$}$$

Given our assumptions on $\mathcal{X}$ and f_i, problem $S(\pi)$ is a mixed-integer linear program (MILP). Its size scales with the number of policy parameters and outcomes, as well as the parametric complexity of the surrogate models. In our implementation (Section 4.1), the relatively small number of parameters and outcomes (in the tens) resulted in MILPs that could be solved to optimality in seconds by general, open-source MILP solvers.

The solution of $S(\pi)$ is ultimately evaluated with a single query of B and its true outcomes computed. Due to errors in the approximation models, it is not guaranteed that the solution is in fact feasible for $P(\pi)$. However the magnitude of constraint violations, if any, is not expected to be large if the surrogates are accurate. Should the violations prove unacceptably large, a safety term could be added to the approximation introducing some slack (see Appendix A).

Finally, we note that, based on the choice of $\boldsymbol{b}$, $S(\pi)$ could be infeasible—indicating that the desired requirements $\boldsymbol{b}$ were overly stringent. To address this possibility, the model can be readily modified using slack variables, and appropriately reformulated to produce a feasible solution that comes "as close as possible" to meeting the requirements $\boldsymbol{b}$. For example, after adding slack variables to each constraint, the objective value of $S(\pi)$ can be reformulated as minimizing the sum of of the slack variables—the original objective can also be used in that case within a constraint, using an epigraph formulation, in which the objective value is constrained to be less than or equal to the minimum value it could attain, plus another slack variable. Depending on the tolerance of violation for each constraint, associated weights can be used to mix the slacks in the objective. We formalize this in Appendix B.

3.3. Implications for Policy Design

There are several important advantages to our optimization approach. First, it enables policymakers to dynamically explore the space of policies and outcomes as they iterate towards consensus. The formulation of problem instances might be implemented as an interactive application, allowing users to intuitively and flexibly define the objective and constraints for their outcomes of interest. Once the instance of interest has been specified, the application will automatically formulate and solve the corresponding MILP to display optimized policy parameters and their simulated outcomes. As a result, stakeholders, even those without technical expertise, can efficiently explore different policy options and refine their value judgments on relevant tradeoffs.

To exemplify, without our framework, policymakers for lung allocation would need to contemplate and debate how much weight to award for each CAS attribute, thereby "mixing apples & oranges" with limited intuition. Within our framework, policymakers can instead focus on debating appropriate target outcomes; a setting where ethical theory and community sentiment is more likely to generate useful feedback.

In particular, policymakers might iteratively solve multiple $P(\pi)$ to produce policies with varying efficiency/fairness characteristics. If a generated policy exhibits some undesirable characteristic, e.g. an unintended increase in transplant rate disparities for patients of different blood types, a constraint on that outcome could be added to the optimization to address it. Conversely, policymakers might perform sensitivity analysis by removing or

modifying a particular constraints to see how other outcomes are affected; for example, does loosening an equity constraint decrease waitlist mortality, and if so by how much?

More generally, our framework allows for global tradeoff analysis. By systematically varying the constraint bound on one outcome (e.g., organ transport distance) while optimizing a second (e.g., minimizing waitlist mortality), policymakers can visualize the (approximate) efficient frontier of outcomes. Critical points, where marginal gains in one outcome diminish significantly relative to another, can provide guidance for how to balance different objectives. Crucially, the advantage of an optimization-based approach here is that policies on the tradeoff curves might be additionally constrained. For example, policymakers might examine the tradeoff in transport distance and waitlist mortality, while ensuring that transplant rate disparities for different subpopulations do not exceed a certain level.

4. Reshaping National Lung Allocation Policy

We discuss how we collaborated with UNOS to apply our framework to the design of a continuous distribution policy for lung allocation. Among others, we performed tradeoff analyses to address two questions confronting the OPTN Lung Transplantation Committee during the policy development process: (i) how to reconcile the Final Rule's competing mandates of placement efficiency and broader geographic distribution to the most urgent patients, and (ii) how to ensure that pediatric patients maintained the same high level of access to organs as they do under the current classification-based system.

Both of these questions have far-reaching implications for fairness, equity, and the welfare of patients, as we discuss next. In particular, the first question has been at the forefront of policy debate for decades (see Section 2.2), and in fact served as a primary motivation for the OPTN's decision to migrate all organ allocation to continuous distribution. Under continuous distribution, the relative weight of placement efficiency in the CAS formula controls the level of geographic distribution. It thus directly encodes the tradeoff between increased transportation burden on the one hand, and waitlist mortality and geographic equity on the other. To this end, we generated tradeoff curves for waitlist mortality vs. various transportation burden metrics, identifying critical points that could guide the committee's selection of a weight for placement efficiency.

The second question reflects the committee's desire to ensure high levels of access for pediatric patients (aged less than 18 years). Beyond ethical motivations for prioritizing this

vulnerable population, pediatric patients are also generally considered medically harder to match due to organ size compatibility constraints. Under the previous classification-based system, pediatric patients formed the highest-priority group for organs recovered from pediatric donors, ensuring that they were offered compatible organs at a high rate. Under continuous distribution, the committee sought to identify the minimum value for pediatric weight that would result in the highest possible transplant rates for pediatric patients, and our framework was applied to this end.

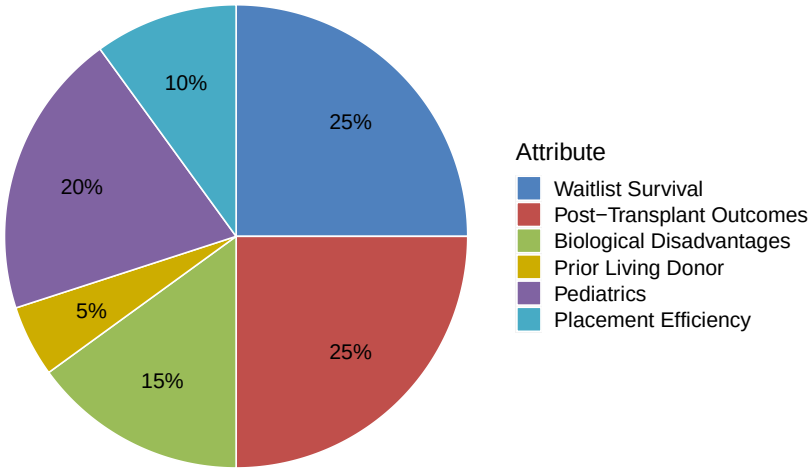

Figure 1 Continuous distribution attribute weights used in the OPTN Lung Transplantation Committee's proposal. Source: reproduced from LTC (2021d).

The results of our analyses, which we detail in the following sections, were presented to the OPTN Lung Transplantation Committee in March 2021 (LTC 2021a,b). We identified 10% placement efficiency weight as a critical point in the tradeoff of waitlist mortality vs. transportation burden, and a range of 15%-20% pediatric weight as the minimum necessary to maintain high levels of pediatric access. Further analysis that we performed, but do not include here, informed the choice of the biological disadvantages attribute weight. After independent validation of our results by the SRTR (2021a), the Committee eventually adopted our recommendations for the placement efficiency, pediatric access, and biological disadvantages weights. In particular, the committee's official continuous distribution proposal, depicted in Figure 1, recommended values of 10% and 20% respectively

for the placement efficiency and pediatric attributes. The proposal was distributed for public comment in August of 2021 (LTC 2021d), ratified in October of the same year (LTC 2021c), approved by the OPTN Board of Directors in December 2021 (OPTN 2021b), and implemented as national policy on March 9, 2023, dictating how deceased-donor lungs are allocated across the U.S. for years to come.

The new policy was independently assessed through simulations performed by the SRTR (2021a). Among other findings, for the new policy, SRTR reported that the number of waitlist deaths declined considerably, and although median distances increased, overall percent of organs expected to fly declined compared with current rules. Further, transplant rates increased considerably for pediatric candidates, especially those aged 12-17, increased more modestly for candidates aged 18-49, and declined for candidates 65 years or older. Of note, transplant rates increased for Latinos and decreased for white candidates, and declines in waitlist deaths were more pronounced for Latino candidates. We refer the reader to SRTR (2021a) for more details and analyses.

4.1. Modeling Implementation

We first describe the implementation of our framework (Section 3) to the design of a lung continuous distribution policy in more detail. Here, the primary policy parameters to be optimized are the CAS weights λ for the six attributes selected by the committee (Section 2.2). In addition to the attributes themselves, the committee previously worked with UNOS to develop a set of *rating scales*, consisting of linear functions for some attributes and nonlinear functions for others, which translated the inherent value associated with each attribute value to a comparable [0,1] scale (LTC 2021d). Thus, our optimization domain consists of weight vectors λ drawn from the unit simplex, $\mathcal{X} = \{\lambda \in [0,1]^6 : \sum_i \lambda_i = 1\}$, so that candidates' CAS scores also lie on a unit scale $[0,1]$.[2]

The blackbox function B represents the SRTR's Thoracic Simulated Allocation Model (TSAM, Version 2015), which simulates counterfactual allocation of 3,326 recovered lungs to 6,546 waitlist candidates over a two-year period from 2009-2011 (SRTR 2021b). We modify the simulator to accept a CAS weight vector λ as input, and implement a continuous distribution allocation scheme using the committee's selected attributes. The output domain $\mathcal{Y}$ consists of 47 simulated outcomes encompassing a wide range of efficiency, utility

Outcome	R^2
Overall Deaths #	0.98
Overall Transplants #	0.94
Med. Organ Transp. Distance (nm)	0.99
Avg. Organ Transp. Distance (nm)	0.98
Organ Transp. Cost (% of current policy)	0.98
Organs Flown (% of total)	0.99
Overall TX Rate	0.98
TX Rate Disparity - OPO	0.98
TX Rate Disparity - Blood Type	0.98
TX Rate Disparity - Age Group (18+)	0.95
TX Rate Disparity - Birth Sex	0.85
TX Rate Disparity - Race	0.99
TX Rate Disparity - Height Group	0.95

Table 1 Surrogate modeling results for simulated lung allocation outcomes.

and fairness metrics, including waitlist mortality, transplant rates, transport burden and equity measures for different patient classifications (see Appendix D).

We applied the optimization methodology of Section 3.2 as follows:

1. **Sample Design** We sampled 10,000 weight vectors λ uniformly at random from the unit simplex to generate a training dataset (Smith and Tromble 2004). Each generated policy was simulated 20 times, and the average value of each outcome was recorded.
2. **Surrogate Modeling** We fit piece-wise linear surrogate models separately for each outcome. In particular, our hypothesis class consisted of piece-wise convex or concave linear functions, i.e., the minimum or maximum of K affine functions of λ, with parameters θ^i corresponding to the coefficients and intercept of each function. We estimated the best-fit parameters by minimizing a standard ℓ_2 loss, using a random 80-10-10% training/validation/testing split. Best-performing hyper-parameters were selected based on R^2 on the held-out validation set. Appendix C includes further details for the interested reader. Out-of-sample R^2 of the selected models ranged from 0.85-0.99 for all outcomes, with an average of 0.96. Table 1 below summarizes the out-of-sample R^2 for key outcomes—further details and results are given in Appendix D.
3. **Optimization** We used the open-source CBC solver (Forrest et al. 2018) to solve the MILPs resulting from the application. More information on MILP formulations of our chosen surrogate models can be found in Appendix C.

This study used data from the Scientific Registry of Transplant Recipients (SRTR). The SRTR data system includes data on all donor, wait-listed candidates, and transplant recipients in the US, submitted by the members of the Organ Procurement and Transplantation Network (OPTN). The Health Resources and Services Administration (HRSA),

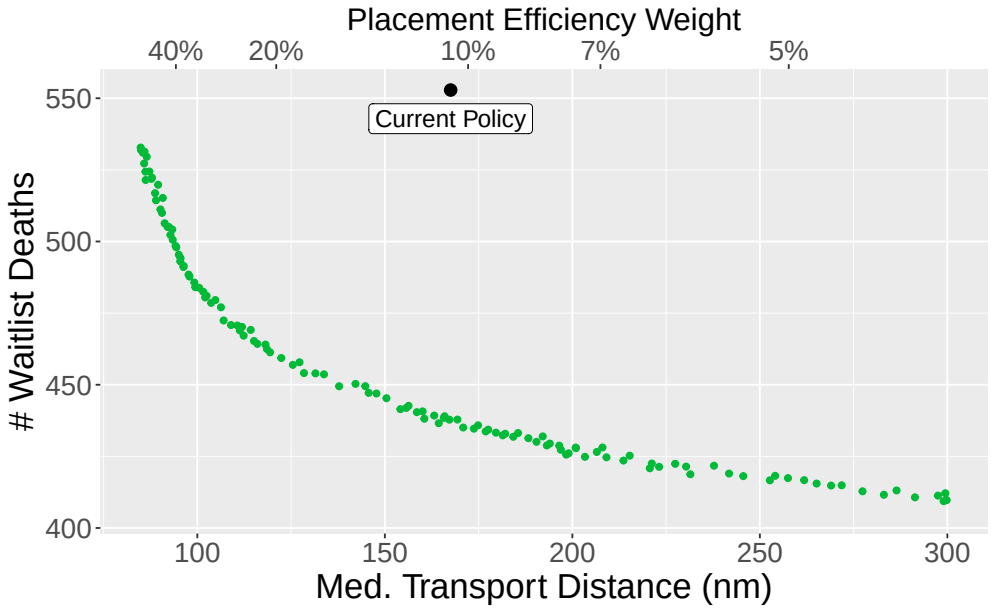

Figure 2 Tradeoff of waitlist mortality and placement efficiency in continuous distribution.

U.S. Department of Health and Human Services provides oversight to the activities of the OPTN and SRTR contractors.

4.2. Tradeoffs for Placement Efficiency

To address the committee's question regarding geographic distribution, we applied our framework to generate tradeoff curves for waitlist mortality and different organ transport metrics. Figure 2 plots the total number of waitlist deaths in simulation vs. median organ transport distance for a series of optimized policies. Each point corresponds to a policy obtained by our model where the objective was to minimize the number of waitlist deaths (y-axis), and the upper bound on transport distance (y-axis) was varied across a grid. All policies used a fixed value of 20% for pediatric access weight (see Section 4.3), and were required to place equal weight on the WLAUC and PTAUC factors (per the committee's guidance). Additional constraints enforced that transplant rate disparities for patients of different blood type and height group did not increase vis-a-vis current policy. At the top of the figure, we mark for certain optimized policies their associated proximity weights. Finally, current policy is also depicted through a distinctively labeled point.

On the left part of Figure 2, we observe policies with a relatively high weight on placement efficiency. These result in higher waitlist mortality as nearby candidates are prioritized more than medically-urgent ones. Moving to the right of the graph, the placement

efficiency weight decreases and organs are allocated to more medically urgent patients who are farther away, decreasing waitlist mortality but increasing transport burden. Of note, we identify a point of diminishing returns at $\approx 10\%$ placement efficiency weight (median organ transport distance of ≈ 175 nautical miles). We observed qualitatively similar results in tradeoff curves for which the x-axis represented two other simulated transport metrics, namely estimated transport cost and percentage of organs expected to be flown, with diminishing returns at around 10% placement efficiency weight (Appendix E).

The robustness of the 10% finding across different transport metrics was independently validated through additional simulations performed by the SRTR on an updated 2018-2019 patient cohort (SRTR 2021a).[3] The final round of official simulation modeling varied placement efficiency weight between of 10%, 15%, and 20%, and confirmed our findings of diminishing returns to waitlist mortality as a function of transport burden, culminating in the committee's official proposal of a 10% weight on placement efficiency (Figure 1). Of note, an optimized CD policy with a 10% placement efficiency weight is seen to reduce waitlist mortality by $\approx 20\%$ compared to current policy in Figure 2, averting ≈ 118 deaths over the 2-year simulation horizon. The SRTR's independent simulation study estimated an even greater reduction of $\approx 40\%$ in waitlist mortality, or 175 deaths averted over a 2-year period.[4] At the same time, it is also more equitable as it no longer relies on hard geographic boundaries in allocation priority.

4.3. Ensuring Pediatric Priority

We also applied our framework to examine the impact of increasing pediatric access weight on pediatric transplant rates. In Figure 3, each point corresponds to an optimized policy with the objective of minimizing pediatric transplant rates (y-axis), while varying the lower bound on pediatric access weight (x-axis). Optimizations were otherwise unconstrained. Thus, the plot shows the worst-case pediatric transplant rate under a continuous distribution policy with a given pediatric access weight, regardless of other requirements.

Figure 3 shows that a pediatric weight of $\approx 10\%$ suffices to ensure that pediatric access stays at the same level as current policy. Moreover, pediatric transplant rate seems to stabilize at a weight of about 15-20%. Although some preliminary, informal analysis by UNOS had suggested that a 30% weight would ensure that pediatric patients were always prioritized above adult patients (maximizing their transplant rate), our results indicate that

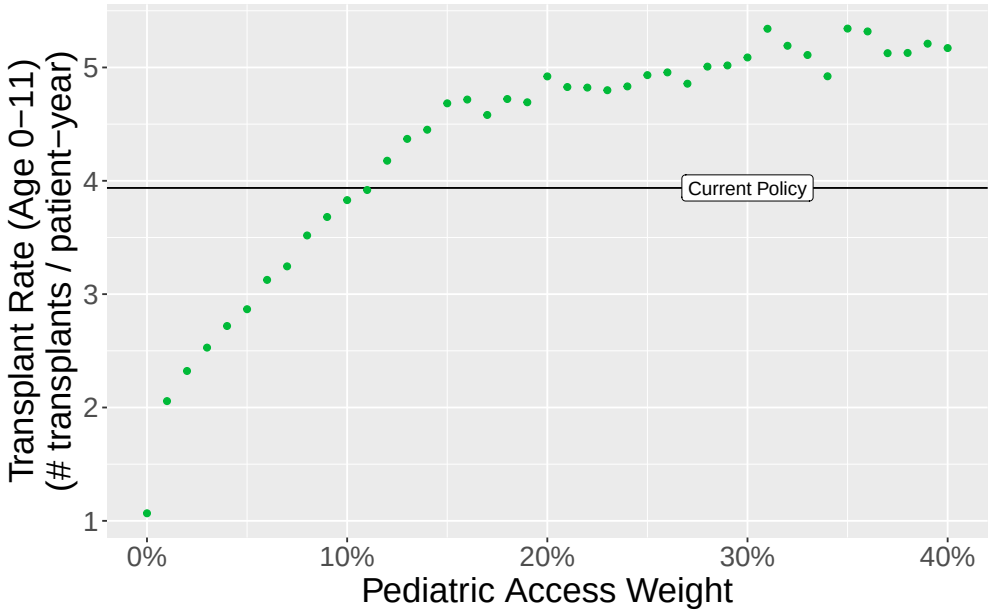

Figure 3 Guaranteed pediatric transplant rate for patients aged 0-11 years vs. pediatric access weight. Rates were similarly evaluated for patients aged 12-17 (Appendix E).

a lower weight sufficed to achieve the same goal. The committee's subsequent simulation requests to the SRTR, as well as their final proposal, fixed pediatric access weight to 20%.

5. Future Opportunities & Limitations

We present a novel analytical framework for multi-objective policy design when prediction of policy outcomes is constrained by a burdensome, non-transparent evaluation process. We leverage machine learning and mixed-integer optimization to enable dynamic design of policies with given outcomes. The result is a flexible decision support tool for policymakers that does not require technical expertise and can be used to understand the range of achievable outcomes and evaluate tradeoffs. One of the chief advantages of this approach is that it enables stakeholders and community groups to offer input at precisely the points at which their views have the most value; in determining the set of desired outcomes of a policy, rather than struggling to determine the exact design parameters that achieve them.

We note that the multi-objective policy design setting we address is hardly unique to the organ allocation problem we studied. Our machine-learning and surrogate optimization approach can be readily applied to the design of any type of parametric allocation policy, not just a scoring rule. Beyond organ allocation, policymakers in a broad range of application domains face similar challenges, seeking to model complex system dynamics

and balance multiple objectives. For example, educational districts seek to assign students to schools so as to best balance family preferences, transportation and operational logistics, and equity and diversity requirements. In public housing allocation, newly available units must be assigned to waitlist applicants with diverse preferences, incorporating broader equity and diversity considerations. Our framework might be applied to evaluate tradeoffs in either domain, when policy outcomes depend on assignments made by a computationally-expensive, blackbox algorithm (e.g., mixed-integer matching formulation) with parametrized objective and constraints. Using a meta-optimization tool such as the one we designed, policymakers in school choice or public housing allocation can explore the range of possible outcomes and evaluate tradeoffs in their objectives of choice.

Although we view our approach as a major step forward in effective policy design, we also note that it is subject to certain limitations. First and foremost, for the surrogate optimization step to be effective, accurate blackbox function's predictions are needed. If the latter have limitations or introduce biases, these would be inherited by the machine-learning models we train, eventually inhibiting policy design.

In organ allocation, the Simulation Allocation Models, for example, have proved over the years invaluable tools for policymakers to assess future candidate policies. Although these models are primarily "event-driven" and heavily rely on historical data, they still have algorithms to make counterfactual predictions for certain outcomes, including the transplant program accept/decline decisions for each organ offer; health evolution for candidates when historical data is censored; arrival sequences of donors and candidates; and post-transplant recipient and graft survival times. These algorithms have been fitted to historical data, but they still require assumptions, e.g., the acceptance model assumes stable organ allocation policy, and thus it does not account for behavioural changes to patient or clinician practice when allocation policy changes, which might result in prediction errors (Goldberg et al. 2017, Goel et al. 2018, Lehr et al. 2020). Improving these simulation tools is an important task, but tangential to the focus of our work. Notably, our framework utilizes these models just as an input, so it could readily incorporate any improved or updated versions thereof. In practice, any remaining limitations should be pointed out to stakeholders to avoid overreliance on imperfect predictions, and to allow clinical and subject-matter expertise to influence the conclusions drawn from the tool.

Second, tradeoff analyses of the kind we presented do not come without limitations. Among them is the diminishing ability of the model to retain accurate counterfactual predictions as one considers policies with outcomes that are increasingly different than the current operating point. For the placement efficiency analysis we presented, for example, this would mean that the estimation accuracy could drop as one moves away from the actual median distance of the current policy in the data—although the 10% placement efficiency weight that was chosen does not suffer from that deficiency. Another related limitation could stem from limited accuracy in the blackbox function's predictions. The OPTN data, for example, has limitations, and many latent variables in the system might mean that certain outcomes are harder to predict than others. One notable example are post-transplant outcomes, which tend to rely on unobserved transplant center's expertise. To mitigate this, in our analysis we focused instead on outcomes for which available data suffice for accurate predictions, e.g., waitlist mortality.

Third, surrogate optimization works well only if the trained models are highly accurate approximations of the blackbox function. In our implementation, relatively simple piecewise linear models sufficed to produce extremely high-fidelity approximations; however, other applications might require more complex surrogate models, which may be harder to train and optimize over to achieve similar performance.

Finally, our approach is best suited to application domains where the problem dimension (number of policy parameters and/or outcomes) is not exceedingly high, to ensure both accuracy of the surrogate models with a relatively small number of training samples, as well as reasonable computational overhead when solving repeated mixed-integer programs.

Acknowledgments and Disclaimers

The authors would like to acknowledge the critical role of the OPTN Lung Transplantation Committee, particularly Erika Lease, MD, Chair; and Marie Budev, MD, Vice Chair; in effectively leveraging this work to inform the policy development process.

The data reported here have been supplied by the Hennepin Healthcare Research Institute (HHRI) as the contractor for the Scientific Registry of Transplant Recipients (SRTR). The interpretation and reporting of these data are the responsibility of the author(s) and in no way should be seen as an official policy of or interpretation by the SRTR or the U.S. Government.

Endnotes

[1]Potential recipients are "sensitized" if their immune system makes antibodies against potential donors. Sensitization usually occurs as a consequence of pregnancy, blood transfusions, or previous transplantation. Highly sensitized patients are more likely to reject an organ transplant than are unsensitized patients.

[2]In later analyses, the committee requested that the ratio of WLAUC:PTAUC weights was fixed to either 1:1 or 2:1. In this case, the domain consists of weight vectors λ drawn from the unit simplex in 5 dimensions, and one dimension is split into two weights according to the given fixed ratio.

[3]The updated simulation model and cohort used by the SRTR was not publicly available at the time of this work.

[4]We note that the absolute values of metrics like the number of waitlist deaths from our study cannot be directly compared to the SRTR's, as they simulate allocation in different patient cohorts with different characteristics.

References

Anderson R, Huchette J, Ma W, Tjandraatmadja C, Vielma JP (2020) Strong mixed-integer programming formulations for trained neural networks. *Mathematical Programming* 1–37.

Bertsimas D, Tsitsiklis JN (1997) *Introduction to linear optimization*, volume 6 (Athena Scientific Belmont, MA).

Biggs M, Hariss R, Perakis G (2017) Optimizing objective functions determined from random forests. *Available at SSRN 2986630* .

Deshpande R, Hirose R, Mulligan D (2017) Liver allocation and distribution: time for a change. *Current opinion in organ transplantation* 22(2):162–168.

DHHS (2000) Organ Procurement and Transplantation Network Final Rule. Electronic Code of Federal Regulations, Title 42–Public Health, Chapter I–Public Health Service, Department of Health and Human Services, Subchapter K–Health Resources Development, Part 121.

Forrest J, Ralphs T, Vigerske S, LouHafer, Kristjansson B, jpfasano, EdwinStraver, Lubin M, Santos HG, rlougee, Saltzman M (2018) coin-or/cbc: Version 2.9.9. URL `http://dx.doi.org/10.5281/zenodo.1317566`.

Glazier AK (2018) The lung lawsuit: A case study in organ allocation policy and administrative law. *Journal of Health & Biomedical Law* XIV(1):139–148.

Goel A, Kim WR, Pyke J, Schladt DP, Kasiske BL, Snyder JJ, Lake JR, Israni AK (2018) Liver simulated allocation modeling: were the predictions accurate for share 35? *Transplantation* 102(5):769–774.

Goldberg DS, Levine M, Karp S, Gilroy R, Abt PL (2017) Share 35 changes in center-level liver acceptance practices. *Liver Transplantation* 23(5):604–613.

Koziel S, Leifsson L (2013) *Surrogate-based modeling and optimization* (Springer).

Lehr CJ, Skeans M, Valapour M (2020) Validating thoracic simulated allocation model predictions for impact of broader geographic sharing of donor lungs on transplant waitlist outcomes. *The Journal of Heart and Lung Transplantation* 39(5):433–440.

LTC (2019) Public Comment Proposal: Establish Continuous Distribution of Lungs. https://optn.transplant.hrsa.gov/media/3111/thoracic_publiccomment_201908.pdf, organ Procurement & Transplantation Network, Thoracic Organ Transplantation Committee. Online; accessed 8 November 2021.

LTC (2021a) OPTN Lung Transplantation Committee Meeting Summary, March 25, 2021. https://optn.transplant.hrsa.gov/media/4567/20210325_lung_meeting_summary.pdf, online; accessed 8 November 2021.

LTC (2021b) OPTN Lung Transplantation Committee Meeting Summary, March 31, 2021. https://optn.transplant.hrsa.gov/media/4579/20210331_lung-meeting-summary.pdf, online; accessed 8 November 2021.

LTC (2021c) OPTN Lung Transplantation Committee Meeting Summary, October 22, 2021. https://optn.transplant.hrsa.gov/media/203b23pe/20211022_lung-committee-meeting-summary_draft.pdf, online; accessed 8 November 2021.

LTC (2021d) Public Comment Proposal: Establish Continuous Distribution of Lungs. https://optn.transplant.hrsa.gov/media/4772/continuous_distribution_of_lungs-public_comment.pdf, organ Procurement & Transplantation Network, Lung Transplantation Committee. Online; accessed 8 November 2021.

Maragno D, Wiberg H, Bertsimas D, Birbil SI, den Hertog D, Fajemisin A (2021) Mixed-integer optimization with constraint learning.

Massie AB, Roberts JP (2018) Geographic disparity in liver allocation: time to act or have others act for us. *Transplantation* 102(2):189–190.

McKay MD, Beckman RJ, Conover WJ (1979) A comparison of three methods for selecting values of input variables in the analysis of output from a computer code. *Technometrics* 21(2):239–245, ISSN 00401706, URL http://www.jstor.org/stable/1268522.

Mišić VV (2020) Optimization of tree ensembles. *Operations Research* 68(5):1605–1624.

Moore LP, Weimer DL (2021) The geography of life and death: Evidence and values in the evolution of us liver transplant rules. *World Medical & Health Policy* .

Murphy KP (2012) *Machine learning: a probabilistic perspective* (MIT press).

OPTN (2018) Executive Summary of the OPTN/UNOS Board of Directors Meeting, December 3-4, 2018. https://optn.transplant.hrsa.gov/media/2787/board_executivesummary_201812.pdf, organ Procurement & Transplantation Network. Online; accessed 8 November 2021.

OPTN (2021a) 10-Step Policy Development Process. https://optn.transplant.hrsa.gov/media/3115/optn-policy-development-process-explanatory-document.pdf, organ Procurement & Transplantation Network. Online; accessed 8 November 2021.

OPTN (2021b) Executive Summary of the OPTN/UNOS Board of Directors Meeting, December 6, 2021. https://optn.transplant.hrsa.gov/media/g23hdtxk/20211206-optn-bod-summary.pdf, organ Procurement & Transplantation Network. Online; accessed 12 January 2022.

OPTN (2021c) Organ Procurement & Transplantation Network Policies. https://optn.transplant.hrsa.gov/media/eavh5bf3/optn_policies.pdf, online; accessed 8 November 2021.

RFI (2008) Kidney Allocation Concepts: Request for Information. https://asts.org/docs/default-source/optn-unos/proposed-kidney-allocation-concepts-rfi-september-24-2008.pdf, OPTN/UNOS Kidney Transplantation Committee. Online; accessed 8 November 2021.

Smith NA, Tromble RW (2004) Sampling uniformly from the unit simplex. *Johns Hopkins University, Tech. Rep* 29.

SRTR (2021a) Continuous distribution simulations for lung transplant: Round 2. https://optn.transplant.hrsa.gov/media/4646/lu2021_01_cont_distn_report_final.pdf, scientific Registry of Transplant Recipients. Online; accessed 8 November 2021.

SRTR (2021b) Simulated Allocation Models. https://www.srtr.org/requesting-srtr-data/simulated-allocation-models/, scientific Registry of Transplant Recipients. Online; accessed 8 November 2021.

Stegall MD, Stock PG, Andreoni K, Friedewald JJ, Leichtman AB (2017) Why do we have the kidney allocation system we have today? a history of the 2014 kidney allocation system. *Human immunology* 78(1):4–8.

Yang Z, Gerull WD, Gauthier JM, Meyers BF, Kozower BD, Patterson GA, Nava RG, Hachem RR, Witt CA, Byers DE, et al. (2020) Shipping lungs greater distances increases costs without cutting waitlist mortality. *The Annals of Thoracic Surgery* 110(5):1691–1697.

Zabinsky ZB, Smith RL (2013) *Hit-and-Run Methods*, 721–729 (Boston, MA: Springer US), ISBN 978-1-4419-1153-7, URL http://dx.doi.org/10.1007/978-1-4419-1153-7_1145.

Theodore Papalexopoulos received his Ph.D. in Operations Research from the Massachusetts Institute of Technology in 2022. His research interests include multi-objective optimization, simulation, and machine learning, and their applications to healthcare and public policy. His Ph.D. thesis focused extensively on organ allocation policy design for the U.S. transplantation system.

James Alcorn is the senior policy strategist with the United Network for Organ Sharing (UNOS), the non-profit leading the U.S. organ donation and transplantation system. In his role, he is responsible for the development of the continuous distribution of organs and setting strategy for how the country determines how to allocate donated organs for transplant in accordance with federal laws and regulations, engaging with medical professionals, patients, academics, institutions, government entities and the public to meet this need.

Dimitris Bertsimas is associate dean of business analytics, Boeing Professor of Operations Research, and faculty director of the Master of Business Analytics at Massachusetts Institute of Technology. His research interests include optimization, machine learning, and applied probability and their applications in healthcare, finance, operations management, and transportation. He has co-authored more than 200 scientific papers and four graduate-level textbooks.

Rebecca Goff is a Manager, Research Science and Biostatistician at the United Network for Organ Sharing. Her research interests include heart and lung transplantation.

Darren Stewart is Associate Director of Registry Studies in the Center for Surgical & Transplant Applied Research (C-STAR) at NYU Langone Health. He leads and conducts scientific studies in the field of organ transplantation.

Nikolaos Trichakis is Associate Professor of Operations Management at Massachusetts Institute of Technology. His research interests include fairness and ethics in analytics, optimization, healthcare and supply chain management.

Appendices

Appendix A: Robustness to surrogate model approximation error

As mentioned in Section 3.2.3, the optimal solution to the surrogate optimization $S(\pi)$ might not in fact be feasible for the instance $P(\pi)$, due to errors in the surrogate models' approximations. In particular, if surrogate model's prediction f_i for a constrained outcome was an overestimation of the true function's value B_i at the computed solution, then the requirement b_i may be violated. Of course, the magnitude of constraint violations, if any, is not expected to be large if the surrogate models are accurate.

Should the violations prove unacceptably large, we propose adding a safety term to the approximation inspired by robust optimization principles. Given a measure of the approximation error of f_i, e.g., the out-of-sample Root Mean Squared Error (rMSE), we make the requirement on outcome i stricter by replacing the constraints in $S(\pi)$ by:

$$f_i(\mathbf{x}\,;\,\boldsymbol{\theta}^i) + \gamma\epsilon_i \leq b_i,$$

where γ is a hyper-parameter controlling the level of conservatism. Higher values of γ make the model more robust to approximation errors, but they also decrease the feasible space and might result in sub-optimality in the objective.

Appendix B: Reformulation of infeasible surrogate optimization

As mentioned in Section 3.2.3, it may be the case that a set of desired outcomes, given by the requirement vector $\boldsymbol{b}$, might be too stringent, rendering the surrogate optimization problem $S(\pi)$ infeasible. To address this possibility, we formulate a modified problem $\hat{S}(\pi)$, where slack variables allow the optimizer to selectively violate constraints, and seek to minimize the total amount of violation.

We first perform a pre-processing step that serves to standardize the requirement vector $\boldsymbol{b}$, so that constraint violations for outcomes with different numerical scales are comparable. We use the sampled dataset $\{\mathbf{x}^n, \mathbf{y}^n\}_{n=1}^N$ from the *Sample Design* phase (Section 3.2.1), to compute lower and upper bounds for each outcome $i \in [d]$, namely $l_i := \min_n y_i^n$ and $u_i := \max_n y_i^n$. The bounds are informal in the sense that they do not constitute explicit constraints on an outcome, but are rather used to gain a sense of its range across the "representative" samples used to train the surrogate models. In particular, they allow us to rewrite requirements b_i in terms of a unitless quantity σ_i:

$$\sigma_i := \frac{b_i - l_i}{u_i - l_i}.$$

Intuitively, σ_i encodes the requirement on outcome i as a relative distance to its minimum/maximum. Typically, we expect σ_i to lie in the interval $[0,1]$ as requirements should be achievable by some point in the domain; however, our approach does not depend on this is as an assumption.

Since l_i and u_i can be computed during the sample design phase, and are therefore fixed at optimization time, $S(\pi)$ is exactly equivalent to:

$$\begin{aligned} \min_{\mathbf{x}\in\mathcal{X}} \quad & f_j(\mathbf{x}\,;\,\boldsymbol{\theta}^j) \\ \text{s.t.} \quad & f_i(\mathbf{x}\,;\,\boldsymbol{\theta}^i) \le l_i + \sigma_i(u_i - l_i) \quad \forall\, i \neq j, \end{aligned} \tag{$S'(\pi)$}$$

where all requirements b_i have been replaced by their relative counterparts σ_i. We emphasize that the optimization problem has not changed. In particular, that if $S(\pi)$ is infeasible then so is $S'(\pi)$.

If this is the case, we can now introduce a modified formulation of $S'(\pi)$ whose optimal solution deviates from the given requirements in some minimum sense, and has a trivially non-empty feasible set:

$$\begin{aligned} \min_{\mathbf{x}\in\mathcal{X},\boldsymbol{s}\ge 0} \quad & \sum_{i=1}^{d} s_i \\ \text{s.t.} \quad & f_i(\mathbf{x}\,;\,\boldsymbol{\theta}^i) \le l_i + (\sigma_i + s_i)(u_i - l_i) \quad \forall\, i \neq j \\ & f_j(\mathbf{x}\,;\,\boldsymbol{\theta}^j) \le l_j + (0 + s_j)(u_j - l_j). \end{aligned} \tag{$\bar{S}(\pi)$}$$

Here we've introduced slack variables $\mathbf{s} \in \mathbb{R}^d_+$. Intuitively, s_i is a decision variable that is added to the relative requirement σ_i, allowing the optimizer to loosen any constraint at its discretion. The objective seeks to minimize the total amount of slack, i.e. the sum total deviation from the desired constraints. Because the relative requirements σ_i are on the comparable scale induced by the ranges (l_i, u_i), minimizing the sum of slacks does not unduly prioritize outcomes with a larger magnitude.

The second constraint provides necessary incentive to minimize the primary objective j, albeit indirectly. Intuitively, the objective's relative requirement is set to $\sigma_j = 0$, and also adjusted by some positive slack, denoting that the outcome should deviate minimally from the lower bound l_j that was observed over the entire dataset.

Appendix C: Surrogate Modeling Implementation

As described in Section 3.2.2, the *Surrogate Modeling* phase of our optimization methodology involves fitting Mixed-Integer Linear Programming (MILP)-representable surrogate models to approximate the blackbox function B. We use machine learning to predict each output of B individually, fitting a parametric approximation $f_i(\boldsymbol{x}\,;\,\boldsymbol{\theta}^i) \approx B_i(\boldsymbol{x})$ for each $i \in [d]$ using the sampled dataset from the *Sample Design* phase.

Concretely, in our lung allocation case study, we fit a model to predict each simulated outcome (e.g., number of waitlist deaths, average organ transport distance) as a function of the CAS scoring weights λ. In what follows we mathematically describe the hypothesis class we used in our implementation, explain the fitting procedure, and formulate the MILP representation of these functions.

C.1. Hypothesis Class

In our lung allocation implementation, we use a hypothesis class of functions we term *affine extremum functions*. These functions are the point-wise minimum or maximum of K affine transformations of the input. Mathematically, given an input $\boldsymbol{x} \in \mathcal{X} \subseteq \mathbb{R}^p$, we fit models of the form:

$$f_i(\boldsymbol{x};\boldsymbol{\beta}) = \max_{k=1,\dots,K}\{\beta_{0,k} + \boldsymbol{\beta}_k^\top \boldsymbol{x}\} \qquad \text{or} \qquad f_i(\boldsymbol{x};\boldsymbol{\beta}) = \min_{k=1,\dots,K}\{\beta_{0,k} + \boldsymbol{\beta}_k^\top \boldsymbol{x}\}. \tag{EC.1}$$

We refer to whether the left (max) or right (min) version is used as the function's *sense* (note that this is not the same the sense of an outcome in our general optimization framework, defined in Appendix B). This class of functions is piece-wise linear over $\boldsymbol{x}$ (and therefore MILP-representable, as we show below), and its members are convex/concave depending on their sense. For simplicity in exposition, we refer to each affine transformation $\beta_{0,k} + \boldsymbol{\beta}_k^\top \boldsymbol{x}$ as a "piece" of the overall function.

The sense and number of pieces K are hyper-parameters, to be selected through cross-validation. For fixed sense and K, there are a total of $K \cdot (p+1)$ parameters that need to be estimated, consisting of a linear coefficient vector $\boldsymbol{\beta}_k \in \mathbb{R}^p$ and intercept $\beta_{0,k}$ for each of the K pieces. We use shorthand $\boldsymbol{\beta}$ to refer to a concatenation of all these parameters.

C.2. Fitting Procedure

During model fitting, we estimate $\boldsymbol{\beta}$ using standard supervised machine learning techniques. We use the dataset generated during the Sample Design phase (Section 3.2.1) to create a dataset for each individual outcome, denoted by $\mathcal{D}_i = \{\boldsymbol{x}^n, y_i^n = B_i(\boldsymbol{x}^n)\}_{n=1}^N$. We randomly split $\mathcal{D}_i$ into training $\mathcal{D}_i^{\text{train}}$, validation $\mathcal{D}_i^{\text{val}}$ and testing $\mathcal{D}_i^{\text{test}}$ sets, using an 80%-10%-10% split.

For a function of the form (EC.1) with fixed K and sense, we estimate best-fit parameters on $\mathcal{D}_i^{\text{train}}$ by minimizing standard ℓ_2 loss:

$$\min_{\boldsymbol{\beta}} \quad \sum_{n=1}^{|\mathcal{D}_i^{\text{train}}|} \left(y_i^n - f_i(\boldsymbol{x}^n;\boldsymbol{\beta})\right)^2.$$

Both inputs and outputs are rescaled to have zero mean and unit standard deviation over the training set to improve numerical performance. Optimization is performed using (sub-)gradient descent with random restarts, starting the procedure from 10 randomly initialized $\boldsymbol{\beta}$ and picking the final iterate that achieved minimum training error. We implement fitting in the Julia programming

language, version 1.1.0, computing gradients using the `ForwardDiff` package and using the gradient descent implementation of the `Optim` package.

We use cross-validation to select the best-performing hyper-parameters (K and sense). For each individual outcome, we search over a grid of K and sense, and select the model trained on $\mathcal{D}_i^{\text{train}}$ that achieved the maximum validation set R^2 on $\mathcal{D}_i^{\text{val}}$. We compute out-of-sample R^2 for the selected model on the test set $\mathcal{D}_i^{\text{test}}$ to evaluate the model's true performance, and retrain on the full dataset $\mathcal{D}_i$ for use in the optimization.

C.3. MILP Formulation

In the *Optimization* phase (Section 3.2.3), we formulate problems $S(\pi)$ where (multiple) surrogate models of the form (EC.1) appear in the objective and constraints, depending on the problem instance π. We present here the MILP formulation for a model with *maximum* sense (first option in Equation EC.1), and note that the other case is similar up to some signs. The full formulation of $S(\pi)$ is obtained by combining the surrogate formulations of all relevant outcomes.

Consider a trained surrogate $f_i(\boldsymbol{x};\boldsymbol{\beta}) = \max_{k=1,\dots,K}\{\beta_{0,k} + \boldsymbol{\beta}_k^\top \boldsymbol{x}\}$ with fixed K. At optimization time, model parameters $\boldsymbol{\beta}$ are fixed to their trained values, while inputs $\boldsymbol{x}$ are decision variables. Our goal is to model a decision variable $y \in \mathbb{R}$ so that, in any feasible solution, $y = f_i(\boldsymbol{x};\boldsymbol{\beta})$. We use the following big-M formulation to linearize the function, introducing binary auxiliary variables $z_k \in \{0,1\}$ for all $k \in [K]$:

$$\sum_{k=1}^{K} z_k = 1 \tag{EC.2}$$

$$y \geq \beta_{0,k} + \boldsymbol{\beta}_k^\top \boldsymbol{x} \qquad \forall k \in [K] \tag{EC.3}$$

$$y \leq \beta_{0,k} + \boldsymbol{\beta}_k^\top \boldsymbol{x} + M(1 - z_k) \qquad \forall k \in [K], \tag{EC.4}$$

where M is some sufficiently large fixed value (see below). Intuitively, the binary variables z_k encode which of the K pieces achieves the maximum value for a given $\boldsymbol{x}$; that is, in any feasible solution we have $z_k = 1$ if $\boldsymbol{\beta}_k^\top \boldsymbol{x} = \max_{k'} \boldsymbol{\beta}_{k'}^\top \boldsymbol{x}$ and 0 otherwise. Constraint EC.2 naturally enforces that one of the pieces must achieve the maximum. Constraints EC.3 ensure that y is lower bounded by the value of each piece, and is therefore greater than their maximum. Finally, Constraints EC.4 upper bound y to enforce exact equality to the maximum piece; that is, for $\{k : z_k = 1\}$ the upper bound matches the lower bound, while the remaining upper bounds are assumed to be even greater for large enough M.

For the formulation to be valid then, M must be selected so that, for *any* $\boldsymbol{x}$ in the domain, the upper bounds for the non-maximum pieces do not conflict with the maximum lower bound. In our implementation, we compute a value for M during pre-processing as follows:

$$M = \max_{k,k'} \max_{\boldsymbol{x} \in \mathcal{X}} \left\{ (\beta_{0,k} + \boldsymbol{\beta}_k^\top \boldsymbol{x}) - (\beta_{0,k'} + \boldsymbol{\beta}_{k'}^\top \boldsymbol{x}) \right\}.$$

In short, we compute the maximum difference between any two pieces over the entire domain $\mathcal{X}$. We note that, when $\mathcal{X}$ is a continuous domain (as in our case), the inner optimization (i.e. for fixed k, k') is a simple linear program (LP). We can than obtain a suitable value for M by solving $(K^2 - K)$ LPs, one for each pair of pieces, and take the maximum objective values as M.

C.4. Derived Models: Mean Absolute Deviation

In our lung allocation implementation, certain outcomes of interest were defined as mathematical functions of other outcomes. Specifically, transplant rate disparities for a given patient classification (e.g., by patient blood type) were defined as the Weighted Mean Absolute Deviation (WMAD) of the individual transplant rates of each relevant subclass of patients (blood type A, B, AB and O), weighted by number of candidates in that subclass (see Appendix D for more details).

For the purposes of optimization, we found that modeling this dependence explicitly in the MILP formulations yielded better performance (i.e. more accurate surrogate optimization) than training a new surrogate model for the disparity metric. More concretely, instead of fitting an affine extremum model to directly predict a WMAD-based disparity metric, we create what we refer to as a *derived* surrogate model, whose prediction is obtained by first calculating transplant rate predictions for each subclass (from the corresponding surrogate models) and subsequently computing their WMAD.

Mathematically, suppose y_j, $j \in [J]$ are the predicted transplant rates for J classes of patient. The derived surrogate model that predicts transplant rate disparities among the classes is defined as:

$$y = \text{WMAD}(y_1, \ldots, y_J) = \frac{1}{J} \sum_{j=1}^{J} w_j \left| y_j - \frac{1}{J} \sum_{j=1}^{J} w_j y_j \right|, \tag{EC.5}$$

where $|\cdot|$ is the absolute value operator, and w_j is a weight associated with the j'th class (e.g., percentage of total population corresponding to the class). Weights are assumed to sum to one, i.e. $\sum_j w_j = 1$.

To use the derived model during optimization, our goal is to model a decision variable $y \in \mathbb{R}$ so that in any feasible solution $y = \text{WMAD}(y_1, \ldots, y_J)$. At optimization time, the weights w_j are fixed, while $y_j \; \forall j \in [J]$ are decision variables corresponding to the outputs of other surrogate models (formulated, e.g., as in Appendix C.3). Here, we use common techniques to linearize each absolute value in the sum of equation EC.5, and optimization can proceed via MILP (Bertsimas and Tsitsiklis 1997).

Appendix D: Lung Allocation Simulated Outcomes

Table EC.1 lists the full set of simulated outcomes that were modeled, and therefore allowed to appear in the objective/constraints of our optimization tool during our collaboration with UNOS and the OPTN. More detailed definitions of the outcomes and related terminology are provided in Appendix G. The table includes detailed results from the Surrogate Modeling phase; in particular, for each simulated outcome j it shows:

- The minimum and maximum value observed for the outcome over the training set. These numbers are intended to illustrate the range and scale of values for each outcome.
- The hyper-parameters of the surrogate model that was ultimately selected through cross-validation. Models are labeled by their hyper-parameters, namely whether they used Min/Max sense, and the number of pieces in the affine extremum class (see Appendix C.1). For example, a "Min7" model indicates that the function was the point-wise minimum of 7 affine functions. Outcomes that were defined as the WMAD of other outcomes, i.e., all TX Rate Disparity Outcomes, are labeled as "Derived" (see Appendix C.4).
- The out-of-sample R^2 and root mean squared error (rMSE) of the selected model.

As noted in Section 4.1, our surrogate models exhibit remarkably high out-of-sample R^2's for all outcomes, ranging from 0.85-0.99 with an average of 0.96. Such high fidelity over the entire domain is key in enabling accurate surrogate optimization regardless of the user's desired requirement vector.

Outcome	l_j	u_j	**Model**	**R2**	**rMSE**
Overall Deaths #	904	1305	Max5	0.98	12
Waitlist Deaths #	399	847	Max5	0.98	12
Post-TX Deaths #	445	538	Min9	0.92	5
Overall Transplants #	3414	3496	Min5	0.94	4
Avg. Net Benefit at TX (days)	10.6	58.3	Min9	0.99	1.0
MLaT	36.0	44.1	Min3	0.98	0.3
MLaT Disparity - OPO	1.1	4.2	Min9	0.93	0.2
Med. Organ Transp. Distance (nm)	74.3	726.3	Max9	0.99	12.3
Avg. Organ Transp. Distance (nm)	132.4	849.7	Max9	0.98	15.7
Organ Transp. Cost (% of current policy)	69.9%	216.6%	Max5	0.98	3.0%
Organs Flown (% of total)	49.7%	96.9%	Max5	0.99	0.9%
Overall TX Rate	1.25	1.57	Max5	0.98	0.01
TX Rate Disparity - OPO	0.27	1.35	Max5	0.98	0.03
TX Rate - Blood Type A	0.32	1.36	Max5	0.97	0.04
TX Rate - Blood Type AB	0.27	1.39	Max5	0.97	0.04
TX Rate - Blood Type B	0.88	1.48	Max5	0.89	0.03
TX Rate - Blood Type O	1.24	6.81	Max9	0.98	0.12
TX Rate Disparity - Blood Type	0.03	3.15	Derived	0.98	0.06
TX Rate - Age 0-11	0.83	6.28	Min7	0.91	0.19
TX Rate - Age 12-17	1.64	55.26	Min7	0.94	2.65
TX Rate - Age 18-34	1.25	1.96	Max9	0.97	0.02
TX Rate - Age 35-50	1.24	2.00	Max12	0.98	0.02
TX Rate - Age 51-65	0.92	1.49	Max5	0.97	0.02
TX Rate - Age 66+	1.24	1.95	Max5	0.92	0.04
TX Rate Disparity - Age Group (18+)	0.10	0.37	Derived	0.95	0.01
TX Rate - Diagnosis Group A	0.35	1.54	Max5	0.96	0.05
TX Rate - Diagnosis Group B	0.36	1.71	Max5	0.97	0.04
TX Rate - Diagnosis Group C	1.38	2.89	Max7	0.97	0.04
TX Rate - Diagnosis Group D	1.62	3.46	Max7	0.98	0.04
TX Rate Disparity - Diagnosis Group	0.07	1.43	Derived	0.98	0.03
TX Rate - Female	0.97	1.26	Max7	0.99	0.01
TX Rate - Male	1.50	2.01	Min7	0.94	0.02
TX Rate Disparity - Birth Sex	0.22	0.40	Derived	0.85	0.01
TX Rate - Asian	1.39	2.50	Max5	0.95	0.05
TX Rate - Black	1.15	1.67	Max7	0.97	0.01
TX Rate - Hispanic	1.47	2.69	Max5	0.98	0.03
TX Rate - White	1.17	1.59	Max5	0.96	0.02
TX Rate Disparity - Race	0.02	0.22	Derived	0.99	0.00
TX Rate - Height 0-157cm	0.96	2.14	Max7	0.97	0.04
TX Rate - Height 157-163cm	0.81	1.13	Max7	0.97	0.01
TX Rate - Height 163-168cm	0.79	1.37	Max5	0.95	0.03
TX Rate - Height 168-173cm	0.98	1.53	Max7	0.94	0.02
TX Rate - Height 173-178cm	1.38	1.99	Max7	0.91	0.04
TX Rate - Height 178+cm	1.44	4.17	Min5	0.94	0.15
TX Rate Disparity - Height Group	0.12	0.86	Derived	0.95	0.03

Table EC.1 Surrogate modeling results for simulated lung allocation outcomes.

Appendix E: Additional Tradeoff Analyses

In Figure EC.1 we provide two additional plots to evaluate the tradeoff between waitlist mortality and transport burden. The plots exactly parallel Figure 2 from the main paper (see Section 4.2 for details), except that two different transport burden metrics are used in lieu of median organ transport distance in the x-axis: (top) estimated organ transport cost as a percentage of current policy, and (bottom) percentage of organs expected to fly. The non-linear (but monotonic) relationship between the transport metric and placement efficiency in the optimized policies can be seen through markings of certain policies' proximity weights at the top of the graph. Of note, we observe qualitatively similar results in terms of diminishing returns to reducing waitlist mortality as placement efficiency is decreased beyond 10%.

Finally, in Figure EC.2 we plot the worst-case guaranteed transplant rate for adolescent patients aged 12-17 years as a function of the pediatric priority weight, paralleling Figure 3 from the main paper (see Section 4.3 for details). We note that transplant rates are very high for this population due to its relatively small size, which results in short active wait times when they are highly prioritized. A pediatric weight of 2% is already enough to guarantee a greater transplant rate than under current policy.

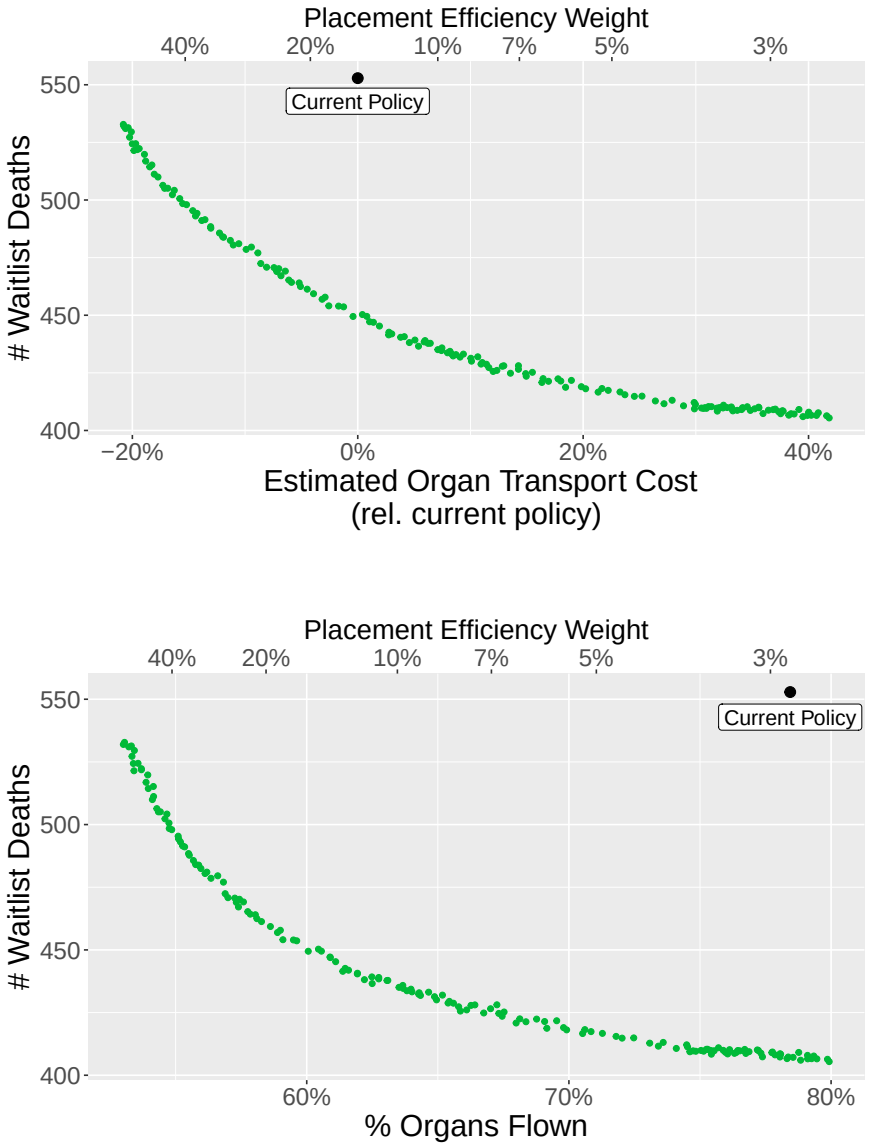

Figure EC.1 Tradeoff of waitlist mortality and placement efficiency in continuous distribution.

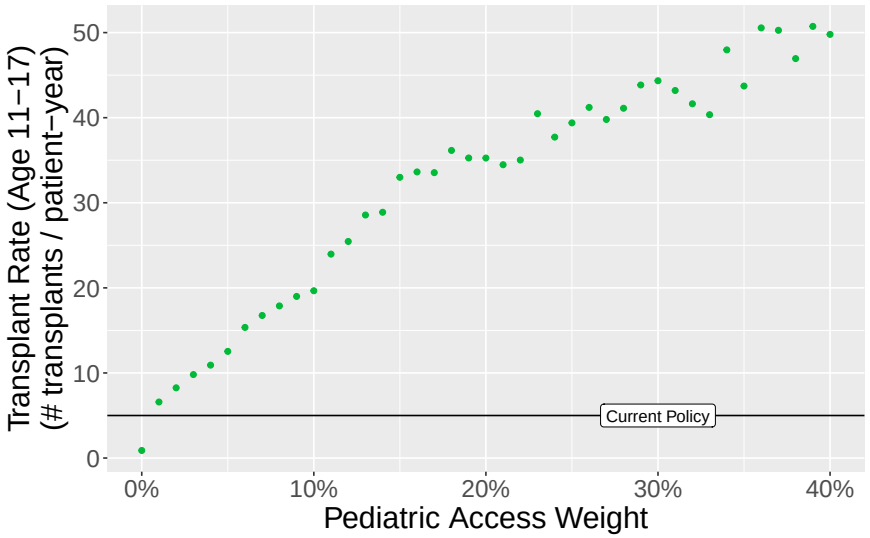

Figure EC.2 Guaranteed pediatric transplant rate for patients aged 12-17 years vs. pediatric access weight.

Appendix F: Replication of Lung Allocation Study

This section outlines the steps needed to replicate the lung allocation analysis presented in this paper, or more generally use our optimization framework to address similar policy design questions in organ allocation.

The first step is to identify the policy parameters that will be optimized under the framework, as well a comprehensive set of policy outcomes that may appear in the objective and constraints (in our case the continuous distribution score weights λ as described in Section 2.2, and the system-wide allocation outcomes listed in Table EC.1 respectively). These decisions are ultimately driven by the needs of the decision-makers, whose expertise can best inform what the measurable characteristics of a well-functioning allocation system are (e.g. low waitlist mortality, equity in access for different blood types, etc.) and what policy levers are available to influence them (e.g. a CAS attribute for medical urgency, an attribute that increases the priority for candidates with a disadvantaged blood type, etc.).

The second step is to identify an effective prediction method for the selected outcomes as a function of the policy parameters. The SRTR's Simulated Allocation Models (SAMs) were a natural starting point for our work as their strengths and limitations have been extensively studied by the transplant community, and used for policy development in the past. In general, we note that the limitations of the prediction method may influence the decisions made in the first step; for example, as noted in Section 5, we focused our optimization and tradeoff analyses on outcomes for which available data and SAM models could provide more accurate predictions (e.g. waitlist mortality).

The SRTR distributes SAMs under a Data Use Agreement (DUA), which includes the software itself, as well as historical transplantation data (candidate/donor cohorts) and statistical models (history generation, offer acceptance, and post-graft survival) used as inputs. For the work presented in this paper, we acquired the 2015 version of TSAM from the SRTR under such a DUA. The only modifications required to replicate this work are: (i) creating Allocation Method input files that define a continuous distribution allocation policy with a given set of score weights λ and the committee's selected CAS attributes, as outlined in LTC (2021d) (ii) modifying the Optional Data Definition input files to create any necessary data transformations (e.g. updated LAS calculation as detailed in OPTN (2021c)) for said attributes. For a given allocation method file, TSAM will then simulate counterfactual allocation and produce output files for each simulated transplant and death that can be aggregated to produce system-wide outcome predictions.

The implementation details of the optimization framework itself, including algorithmic descriptions, hyperparameter choices, and relevant software tools, are detailed in various parts of the

paper. In particular, Section 4.1 and Appendices B and C describe the experimental setup, including training sample size, surrogate model hypothesis class, fitting procedure, MILP formulations, hyperparameter values and software tools. Appendices D and G provide detailed definitions/references for allocation outcome metrics and calculations.

Appendix G: Lung Allocation Glossary

We provide here a glossary of relevant terms and definitions for our lung allocation work. This includes common metrics used to determine patients' allocation priority, as well as measure system-wide outcomes during simulation.

Active patient years: Total active waitlist time for a group of patients, measured in years. For a single patient, active time is measured as time elapsed between their listing (addition to the waitlist) and their removal (due to death, receiving a transplant, becoming too ill to transplant, or other reason), excluding any periods when they were listed as inactive. The total wait time, summed over groups of patients, is used as a normalizing factor to compare transplant/mortality rates across populations with different sizes.

Continuous Distribution (CD): An allocation policy whereby candidates for a given organ are ranked according to Composite Allocation Score that incorporates both patient and donor attributes (see Section 2.2).

Diagnosis Group: A categorization of disease diagnosis for lung waitlist candidates into four broad groups (A, B, C, D). The classification is standard under OPTN Policy.

Lung Allocation Score (LAS): a primary measure of lung allocation priority, used by the OPTN to prioritize lung candidates under current (non-CD) policy (OPTN 2021c). Defined as $\text{PTAUC} - 2 \cdot \text{WLAUC}$, and normalized to lie on a 0-100 scale.

Median LAS at Transplant (MLaT): The median LAS score at time-of-transplant across a group of transplanted patients. Population-weighted Mean Absolute Deviation (WMAD) of MLaT across different OPOS is used as a measure of geographic equity, in the sense that larger variances in MLaT occur when high-LAS (i.e., high urgency/benefit) patients are receiving most transplants in some OPOs but not others.

Net Benefit: A measure of a lung patient's expected benefit from receiving a transplant of median quality, calculated as the difference between their PTAUC and WLAUC at any given point in time. Given the definition of those two metrics, net benefit measures the expected additional days they are expected to live within the next year if they receive a transplant rather than remain on the waitlist. Average net-benefit at time-of-transplant is used as a measure of system-wide utility, in the sense that higher values occur when organs are allocated to patients who would gain the most life expectancy from receiving a transplant.

Organ Procurement Organization (OPO): not-for-profit organizations responsible for recovering deceased-donor organs and collecting patient and donor clinical information to the OPTN. There are 57 OPOs in the United States, each covering different geographic donation service area.

Organ Transport Distance: The geographic distance between the donor hospital where an organ is recovered and the transplant center where a candidate is listed (and would be transplanted

if allocated the organ), measured in nautical miles. Average or median organ transport distance across all transplants is used as a system-wide measure of efficiency, in the sense that higher values indicate higher transport burden.

Organ Transport Cost: The estimated cost of transporting an organ from the donor hospital to the transplant center where a candidate is listed (and would be transplanted if allocated the organ), measured in dollars. In reality, organ transport cost can vary greatly based on circumstance. For the purposes of simulation, an expected cost is calculated as a non-linear function of organ transport distance, according to a model developed by the SRTR. Given the approximate nature of this estimate, we express total transport costs over a simulated period only as a percentage relative the total transport cost estimated for current (non-CD) policy over the same simulated period.

Organs Flown: The number of transplants (expressed as a count or percentage of the total) requiring organ transport by plane. In reality, cases when a recovered organ must be flown can vary greatly based on circumstance. According to UNOS guidance, simulations assumed that an organ would be flown if the distance between the donor hospital and transplant center was greater than 75 nautical miles.

Post-TX Mortality: Patient deaths (expressed as a count, or normalized by total wait time) that occurred due to graft failure after the patient received a transplant. In our simulations, we only consider post-transplant deaths within the first year, as predicted by a survival analysis model included with the version of TSAM we obtained.

PTAUC: "Post-Transplant Area Under (the survival) Curve", a survival analysis-based measure of a lung patient's *post-transplant outcomes*. PTAUC measures the expected number of days the patient is expected to survive within the next year if they receive a transplant of median quality. Its calculation is based on a patient's clinical and demographic data at a given point in time, and is standard according to OPTN Policy (OPTN 2021c).

Transplant Rate (TX Rate): The number of transplants received by a group of patients divided by their total active waitlist time, measured in transplants per patient-year. Transplant rates are reported for six different patient classifications, according to blood type (A, B, O, AB), diagnosis group (A, B, C, D), height sextile (<157cm, 157-163cm, 163-168cm, 168-173cm, 173-178cm, 178cm), age (<12, 12-17, 18-34, 35-50, 51-65, >66 years old), birth sex (Male, Female) and race (Asian, Black, Hispanic, White).

TX Rate Disparity: The Weighted Mean Absolute Deviation (WMAD) of transplant rates of different patient groups, measured in transplants per patient-year (see Section C.4 for a mathematical definition of WMAD). For example, transplant rate disparities by patient blood type would the population-weighted WMAD of transplant rates for patients of type A, B, O and AB. These metrics are used as a system-wide measure of equity by different patient classifications, in the

sense that smaller discrepancies between groups occur when different sub-populations are receiving transplants at similar rates. Weights are included in the calculation, based on the number of patients within each sub-population, so that the measure is not dominated by small groups whose transplant rates tend to be more volatile.

Waitlist Mortality: Patient deaths (expressed as a count, or normalized by total wait time) that occurred while a patient was on the waitlist or after they were removed from the waitlist due to being too ill to receive a transplant.

WLAUC: "Wait List Area Under (the survival) Curve", a survival analysis-based measure of a lung patient's *waitlist urgency*. WLAUC measures the expected number of days the patient is expected to survive within the next year if they remain on the waitlist and do not receive a transplant. Its calculation is based on a patient's clinical and demographic data at a given point in time, and is standard according to OPTN Policy (OPTN 2021c).